Proceedings of the 8th International Symposium on Cavitation
CAV2012 – Submission No. 190
August 13-16, 2012, Singapore

Bubble cluster dynamics in an acoustic field

Elvira S. Nasibullaeva
Center for Micro and Nanoscale Dynamics
of Dispersed Systems, Bashkir State University,
Ufa, 450074, Russia;
Institute of Mechanics, Ufa Branch of Russian
Academy of Sciences, Ufa, 450054, Russia

Yekaterina V. Volkova
Center for Micro and Nanoscale Dynamics
of Dispersed Systems, Bashkir State University,
Ufa, 450074, Russia
Institute of Mechanics, Ufa Branch of Russian
Academy of Sciences, Ufa, 450054, Russia

Nail A. Gumerov
Institute for Advanced Computer Studies,
University of Maryland, College Park, USA;
Center for Micro- and Nanoscale Dynamics
of Dispersed Systems,
Bashkir State University, Ufa, Russia

Iskander S. Akhatov
Department of Mechanical Engineering,
North Dakota State University, Fargo, USA;
Center for Micro- and Nanoscale Dynamics
of Dispersed Systems,
Bashkir State University, Ufa, Russia

SUMMARY

Mathematical model describing the dynamics of a bubble cluster composed of gas bubbles of various radii oscillating in an unbounded, slightly compressible viscous liquid under the action of an external acoustic field is presented. The proposed model is used for an analytical study of small (linear) bubble oscillations in monodisperse and polydisperse clusters, for a numerical investigation of large (nonlinear) bubble oscillations, and for a diffusion stability analysis of gas bubbles in the cluster. The following phenomena have been revealed:

(1) synchronization of the collapse phases of bubbles with different radii;
(2) collapse intensification for bubbles of one size in the presence of bubbles of other size;
(3) bubbles in a monodisperse cluster are more diffusively stable than a single bubble in an infinite liquid;
(4) polydisperse (two-fraction) cluster tends to become a one-fraction cluster due to the diffusion.

INTRODUCTION

Cavitation is the formation of bubble clusters or bubble clouds in a liquid subject to tension. Direct experiments for studying the dynamics of bubbles in clusters or clouds represent a significant technical complexity. Therefore mathematical modeling of the dynamics of bubbles in the cluster is of great importance. One can distinguish two complementary approaches to study bubble clouds:

(1) analysis of dynamics of the bubble cluster in which a mixture of liquid and gas bubbles is considered as a continuum;
(2) analysis of motion of single bubbles in the cluster.

In the first approach the cluster is considered as bubbly liquid. One of the first who considered the dynamics of bubble clusters but was van Wijngaarden [1] who found that the collapse of a large number of bubbles close to a smooth wall leads to increase in pressure near the wall as the result of bubble interactions. After that the bubble cloud dynamics was studied theoretically by many authors (see for example, [2-6].

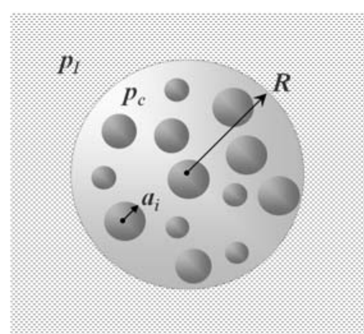

Figure 1: Schematic of a polydisperse bubble cluster.

In this paper the dynamics of a set of gas microbubbles oscillating in a finite volume of an unbounded slightly compressible viscous liquid under the action of an acoustic field is studied. Such a bubble cluster can be pictured as a spherical drop containing a liquid and microbubbles of different initial radii as depicted in Figure 1. This study is further development of the approach proposed earlier in [8, 9, 14, 15].

The main assumptions are following:

(1) the size of the cluster R is small in comparison with the wavelength of the acoustic field in bubbly liquid λ;

(2) the scattering cross sections of neighboring bubbles don't overlap [7] ($\tilde{\sigma}^{1/2} << l$, where $\tilde{\sigma}$ is the value of the bubble scattering cross section; l is the average distance between the bubbles);

(3) the gas pressure inside the bubbles is spatially uniform for each bubble;

(4) bubbles are spherically–symmetric;

(5) there is no liquid evaporation/condensation phase transition in the cluster, the uniform gas pressure inside the bubbles obey the adiabatic law and mass transfer is absent.

Note that under assumptions (1) and (2), the liquid pressure inside the cluster p_c can be considered as *uniform* and time-dependent, i.e. $p_c = p_c(t)$.

MATHEMATICAL MODEL OF BUBBLE CLUSTER

When a polydisperse cluster contains bubbles of n different sizes, the dispersed phase can be divided into n fractions, each characterized by its initial bubble radius (a_{0k} for k-th fraction). The radial motions of a conventional cluster boundary and bubble radii in general case obey the following set of equations ([8], [9]):

$$a_k \ddot{a}_k + \frac{3}{2}\dot{a}_k^2 = \frac{p_{ak} - p_c}{\rho_l}, \quad k = \overline{1,n}, \tag{1}$$

$$R\ddot{R} + \frac{3}{2}\dot{R}^2 = \frac{p_c - p_I}{\rho_l} + \frac{R}{\rho_l C_l}\frac{d}{dt}\left[p_c - p_I\right], \tag{2}$$

$$\sum_{k=1}^{n} N_k a_k^2 \dot{a}_k = R^2 \dot{R}, \tag{3}$$

$$p_{ak} = \left(p_0 + \frac{2\sigma}{a_{0k}}\right)\left(\frac{a_k}{a_{0k}}\right)^{-3\gamma} - \frac{4\mu\dot{a}_k}{a_k} - \frac{2\sigma}{a_k}, \quad k = \overline{1,n}, \tag{4}$$

$$p_I = p_0 - \Delta P \sin(\omega t). \tag{5}$$

Here p_{ak} is the pressure of gas at bubble wall of k-th fraction; p_I is the driving incident pressure; ρ_l is the liquid density; C_l is the sound speed in the liquid; p_0 is the static ambient pressure; ΔP is the pressure amplitude; ω is the driving frequency; σ is the surface tension; μ is the liquid viscosity; γ is the polytropic exponent; N_k is the number of bubbles in the cluster of k-th fraction and t is the time.

The ranges of parameters of applicability of this model have been determined. On Figure 2 two different initial bubble sizes $a_0 = 5$ mkm and $a_0 = 25$ mkm are presented. Areas of mathematical model validity are shaded by parallel lines. The area shaded by parallel vertical lines on Figure 2(b) is an area where a cluster does not exist due to geometrical constraints. Number I denotes the level line $R_0 = \lambda$ (see assumption (1)) and number II shows level curves $\tilde{\sigma}^{1/2} = l$ (see assumption (2)). It is seen that increase of the initial bubble radius from $a_0 = 5$ mkm to $a_0 = 25$ mkm leads to an increase and shift to the areas, where the condition $\tilde{\sigma}^{1/2} << l$ is not satisfied.

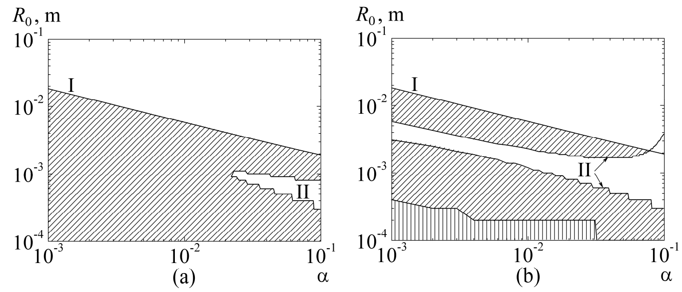

Figure 2: Areas of validity of mathematical model shaded by parallel lines for: (a) $a_0 = 5$ mkm and (b) $a_0 = 25$ mkm. The area shaded by parallel vertical lines indicates the area were no cluster exist with these parameters. Level curves: I – $R_0 = \lambda$; II – $\tilde{\sigma}^{1/2} = l$.

RESULTS

The analytical study of small bubble oscillations based on the bubble cluster model proposed in this paper showed that the natural frequency of bubble oscillations in a monodisperse cluster is expressed by formula

$$\omega_c^2 = \frac{3\gamma p_0 + \dfrac{2\sigma}{a_0}(3\gamma - 1)}{\rho_l a_0^2 \left(1 + N a_0 / R_0\right)} < \omega_M^2,$$

This is lower than the natural frequency of a single bubble (Minnaert frequency) with the same initial radius.

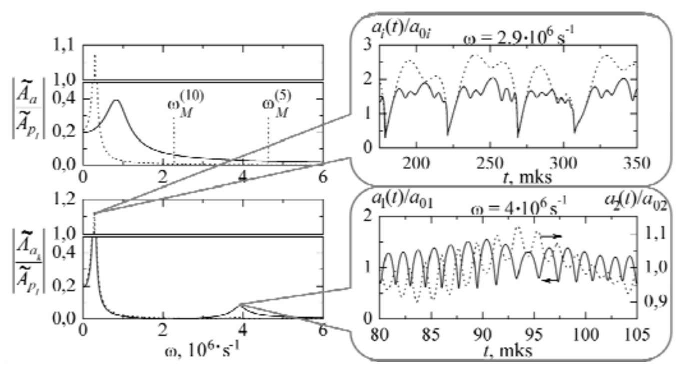

Figure 3: Amplitude-frequency characteristics for monodisperse (top left) clusters with $N = 5000$ each and two-fraction (bottom left) clusters with $N_1 = N_2 = 5000$, and typical bubbles oscillations in two-fraction cluster in the vicinity of the main resonance (top right) and the secondary resonance (bottom right). Vertical dotted lines indicate values of Minnaert frequencies $\omega_M^{(5)}$ and $\omega_M^{(10)}$ for a single bubble of initial radius of 5 mkm and 10 mkm respectively. Solid lines indicate curves for bubble of 5 mkm initial radius; dashed lines indicate curves for bubble of 10 mkm initial radius.

The expression for bubble amplitude as function of frequency where the acoustic field is taken into account has been obtained. Figure 3(left) shows the amplitude-frequency functions for monodisperse cluster (top graph) and two-fraction cluster (bottom graph). Physical parameters correspond to the parameters of air and water: $\rho_l = 10^3$ kg/m^3, $C_l = 1500$ m/s, $p_0 = 10^5$ Pa, $\sigma = 0.073$ N/m, $\mu = 10^{-3}$ Pa·s, $\gamma = 1.4$. Initial cluster radius is $R_0 = 10^{-3}$ m.

One can see that for two-fraction cluster besides the main resonance, which takes place at low frequency, there is a secondary resonance at higher frequency. Figure 3(right) demonstrates the nature of nonlinear oscillations of bubbles in cluster in an acoustic field of $\Delta P = 5 \cdot 10^5$ Pa in the vicinity of these two resonances. It is seen that in the vicinity of the main resonance (at $\omega = 2.9 \times 10^5$ s^{-1}) bubbles in both fractions oscillate in phase. In the vicinity of the second resonance (at $\omega = 4 \times 10^6$ s^{-1}) they oscillate out of phase, while the period of expansion of bubbles of the first fraction coincides with the period of contraction of bubbles of the second one.

The equations (1–5) have been solved numerically using the Runge-Kutta method based on Dorman-Prince formulas with automatic time-step control [10] for the analysis of nonlinear oscillations of bubbles in the cluster.

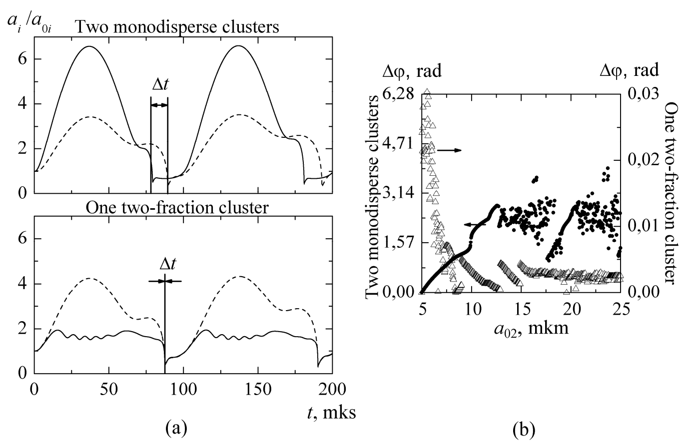

Figure 4: Comparison of bubbles oscillations in two monodisperse and one two-fraction clusters at $\Delta P = 5 \times 10^5$ Pa, $\omega = 2\pi \times 20$ kHz and $N = 10^4$ ($N_1 = N_2 = N/2$):

(a) dependence of the bubble radius vs. time (solid lines for $a_{01} = 5$ mkm, dash lines for $a_{02} = 10$ mkm);

(b) difference of the phases of maximum compression ($a_{01} = 5$ mkm is fixed, a_{02} is variable).

The phenomenon of phase synchronization of bubbles collapse in polydisperse cluster is shown in Figure 4. The Figure 4(a) shows that in two separate monodisperse clusters with different initial bubble radii ($a_{01} = 5$ mkm and $a_{02} = 10$ mkm) the bubbles reach their minimum sizes at different times. But if these bubbles are placed in one cluster making two-fraction cluster, they reach their minimum sizes almost at the same time. Moreover, it is evident that the amplitude of a bubble expansion in the first fraction became lower, while the amplitude of a bubble in the second fraction increased. For clarity there is a graph in Figure 4(b) illustrating the phase difference of the collapse of bubbles of various initial radii calculated by the formulae

$$\Delta\varphi = \varphi_1^{(col)} - \varphi_2^{(col)};\ \ \varphi_k^{(col)} = \omega t_k^{(col)},\ k = 1,2,$$

Here $t_k^{(col)}$ is the time when the bubble of initial radius of a_{0k} reaches its minimal value. The difference between the collapse phases for two monodisperse clusters is shown by dots (left scale), and for two-fraction cluster is shown by triangles (right scale).

Figure 5 shows the phenomenon of an intensification of the bubbles collapse, which is the result of energy exchange between the fractions. Namely, adding a certain number of bubbles with specific radius in the cluster containing bubbles with another radius can lead to a deeper collapse of the latter ones. This result is consistent with experiments [11], where it was found that in a cluster with two bubble sizes, small bubbles collapse deeper in the presence of large bubbles.

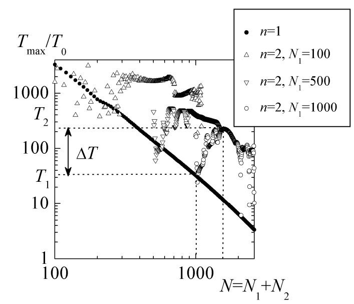

Figure 5: Maximum temperature in the bubble of initial radius of $a_{01} = 5$ mkm vs. total number of bubbles in cluster at $\Delta P = 5 \times 10^5$ Pa. For the case $n = 2$: N_1 is fixed, N_2 is variable, $a_{02} = 10$ mkm.

Let us assume now that the mass transfer due to rectified diffusion is taken into account (assumption (5) is not valid).

Diffusion between the bubble and the liquid is calculated using diffusion averaging approximation developed in [12]. The approximation is carried out for large Peclet numbers ($\mathrm{Pe} = a_0^2\omega / D >> 1$, where D is the diffusion coefficient of gas in liquid) by transforming to the normalized Lagrangian coordinate $\zeta = \left(r^3 - a^3(t)\right) / \left(3a_0^3\right)$, where r is the distance to the centre of the bubble, and by averaging over time.

Then the rate of gas mass transfer through the bubble interface averaged over the period of bubble oscillation is represented as follows:

$$\frac{d\overline{m}}{d\tau} = \frac{\overline{c}_\infty - \langle \overline{c} \rangle_\tau}{T_{rd}}, \qquad T_{rd} = \int_0^\infty \frac{d\eta}{\frac{1}{T}\int_0^T \left[3\eta + \overline{a}^3(t)\right]^4}, \quad (6)$$

$$\overline{c} = \frac{c(a(t),t)}{c_0},\ \overline{c}_\infty = \frac{c_\infty}{c_0},\ \overline{m} = \frac{m}{m_0},\ \overline{a} = \frac{a}{a_0}.$$

Here $\tau = tD/a_0^2$ is the slow diffusion time scale; T_{rd} is the dimensionless characteristic time of the growth rate of bubble mass due to diffusion; T is the period of external acoustic field; $c(a(t),t)$ is the mass concentration of gas dissolved in the liquid near the bubble interface; c_0 is the saturation concentration of gas in liquid at pressure p_0; c_∞ is the initial uniform concentration of gas in liquid; m_0 is the mass of gas initially dissolved in liquid, which occupies the volume of the undisturbed bubble. Average concentration of gas near the bubble wall for the oscillation period of the acoustic field is determined by the expression

$$\langle \bar{c} \rangle_\tau = \frac{1}{\int_0^T a^4(t)dt} \int_0^T a^4(t)\bar{c}dt \ . \tag{7}$$

Gas concentration dissolved in the liquid at the bubble interface was calculated by the formula

$$c(a(t),t) = H\left(p_0 + \frac{2\sigma}{a_0}\right)\left(\frac{a(t)}{a_0}\right)^{-3\gamma}, \tag{8}$$

where $H = c_0/p_0$ is the Henry constant.

For the numerical calculations of mass transfer through the surface of the bubble in the cluster the approximation formulas (6), (7) are used, where gas concentration near the bubble wall is found from the boundary condition (8) and the radius of the bubble $a(t)$ is found from the solution of the system of equations (1-5) for $n = 1$.

Normalized maximum bubble radius a_{max}/a_0 and curves of the average gas concentration near the bubble wall $\langle \bar{c} \rangle_\tau$ for different amplitudes of the acoustic field ΔP are shown in a Figure 6. Figure 6(b) allows to compare results for a bubble in a monodisperse cluster with similar results for a single bubble (see Figure 6(a)) calculated in [13]. Maximum responses for a bubble in a monodisperse cluster (Figure 6(top)) for the amplitudes of pressure $\Delta P = 1.1 \div 1.5 \times 10^5$ Pa occur for about the same size of initial radius as for a single bubble. However the magnitude of the response is much smaller. For example, at $\Delta P = 1.5 \times 10^5$ Pa resonant radius is about $a_0 \approx 1.5$ mkm both for a single bubble and for a bubble in a cluster, but the value of the response in the former case is 6.5 times larger.

Curves of the averaged gas concentration $\langle \bar{c} \rangle_\tau$ near the bubble interface are shown in a Figure 6(bottom). These curves are calculated by formula (7) for a single bubble (see Figure 6(a)) and for a bubble in the cluster (see Figure 6(b)) depending on the initial bubble radius for different amplitudes of the pressure. In this range of initial radius values the character of curves for the averaged concentration of a bubble in the cluster (see Figure 6(b)) is the same as in the case of a single bubble. Namely, the concentration decreases monotonically while initial radius increases to certain threshold value of the driving pressure amplitude ΔP.

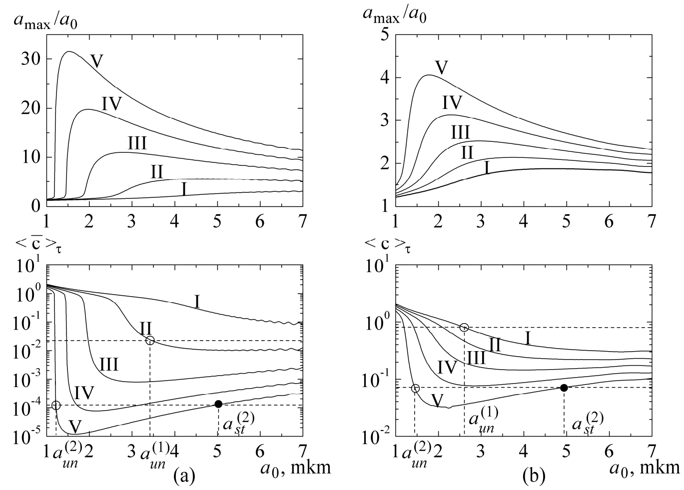

Figure 6: Normalized maximum radius (top) and the average concentration of gas near the bubble wall (bottom), depending on the initial radius for different pressure amplitudes:
(a) single bubble;
(b) bubble in a monodisperse cluster.
Solid curves: I – $\Delta P = 1.1 \times 10^5$ Pa; II – $\Delta P = 1.2 \times 10^5$ Pa; III – $\Delta P = 1.3 \times 10^5$ Pa; IV – $\Delta P = 1.4 \times 10^5$ Pa; V – $\Delta P = 1.5 \times 10^5$ Pa. The horizontal dotted lines represent different levels of initial concentration of gas in a liquid, open circle denotes an unstable equilibrium radius, filled circle denotes a stable equilibrium radius.

The averaged rate of the gas mass in a bubble depends only on the difference between gas concentration in a liquid $\bar{c}_\infty$ and averaged concentration near the bubble interface $\langle \bar{c} \rangle_\tau$ (see formula (6)). There is a range of values $\bar{c}_\infty$ for given pressure amplitudes, when there is one equilibrium point $\langle \bar{c} \rangle_\tau = \bar{c}_\infty$ which is unstable (the open circle at intersection of the curve at $\Delta P = 1.2 \times 10^5$ Pa and the upper dash line). This equilibrium point corresponds to the initial radius value $a_{un}^{(1)}$. For $a_0 < a_{un}^{(1)}$ bubbles dissolve and for $a_0 > a_{un}^{(1)}$ bubbles grow up until they are destroyed by the shape instability. Once the certain threshold value of ΔP is reached the concentration curve $\langle \bar{c} \rangle_\tau (a_0)$ is getting non-monotonous as a result of non-monotonous bubble response shown at the top of Figure 6. With such a non-monotonic dependence $\langle \bar{c} \rangle_\tau$ vs. a_0 there is a range of values $\bar{c}_\infty$ for which there are two equilibrium points $\langle \bar{c} \rangle_\tau = \bar{c}_\infty$. Unstable point (the open circle at intersection of the curve at $\Delta P = 1.5 \times 10^5$ Pa and the under dash line) corresponds to radius $a_0 = a_{un}^{(2)}$ and stable point (the filled circle) corresponds to radius $a_0 = a_{st}^{(2)}$. For $a_0 < a_{un}^{(2)}$ bubbles dissolve until they disappear, for $a_{un}^{(2)} < a_0 < a_{st}^{(2)}$ bubbles grow up until they reach equilibrium radius $a_{st}^{(2)}$ and, finally, for $a_0 > a_{st}^{(2)}$ bubbles dissolve until they reach $a_{st}^{(2)}$. However, the equilibrium in bubble cluster is possible at larger (few hundred times larger) initial concentrations of dissolved gas than in the case of a single bubble. It means that purified liquid separated well from the gas is required to obtain a diffusively stable single bubble, whereas in not purified liquid the appearance of diffusively stable bubble cluster is most likely to occur.

The bubble maximum response and the averaged gas concentration at interface for a bubble initial radius values up to ($a_0 = 1 \div 15$ mkm) for amplitude of the external pressure $\Delta P = 1.5 \times 10^5$ Pa are presented in Figure 7. While initial radius increases the curve of bubble maximum response becomes non-monotonic (Figure 7(top)) and new equilibrium points appear on the curve of averaged gas concentration at interface (Figure 7(bottom)). With further increase in the radius the period doubling bifurcation is observed. The shape of the curve of gas averaged concentration near the bubble interface also changes (Figure 7(bottom)). With period doubling of bubble oscillation the averaged over period of acoustic driving concentration curve is also bifurcates. So averaging over the period of the bubble oscillation (dashed curve) must be performed rather than over the period of the acoustic field. One can see that at low concentrations $\bar{c}_\infty$ there are no equilibrium points at all. With increase of $\bar{c}_\infty$ there are two equilibrium points (stable and unstable). If $\bar{c}_\infty$ increases further then four points of equilibrium appear (two stable and two unstable). This case is shown in Figure 7: filled circles correspond to stable points, open ones correspond to unstable points. Maximum radii corresponding to them are shown by vertical dotted lines. For given values of initial concentration one has the following. For $a_0 < a_{un}^{(1)}$ bubbles dissolve until they completely disappear; for $a_{un}^{(1)} < a_0 < a_{st}^{(1)}$ and $a_{st}^{(1)} < a_0 < a_{un}^{(2)}$ bubbles grow or dissolve, respectively, until they reach an equilibrium size $a_{st}^{(1)}$; for $a_{un}^{(2)} < a_0 < a_{st}^{(2)}$ and $a_0 > a_{st}^{(2)}$ bubbles grow or dissolve, respectively, until they reach an equilibrium size $a_{st}^{(2)}$.

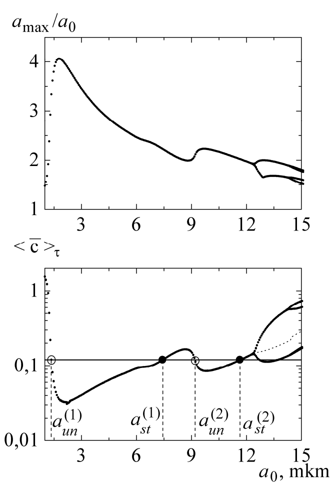

Figure 7: Normalized maximum radius (top) and averaged gas concentration near the bubble wall (bottom) vs. initial radius for pressure amplitude $\Delta P = 1.5 \times 10^5$ Pa.

In case of two-fraction cluster there is an interaction between bubbles of different radii through pressure p_c inside the cluster. Consequently, the averaged gas concentration near the bubble interface for each fraction will depend not only on the radius of the bubble in this fraction, but also on the radius of the bubble in the other fraction. Thus, the averaged gas concentrations near the bubble walls can be represented as a function of two radii:

$$\langle \bar{c}_{a1}(a_{01}, a_{02}) \rangle_\tau, \ \langle \bar{c}_{a2}(a_{01}, a_{02}) \rangle_\tau .$$

For two-fraction cluster at a fixed value of $\bar{c}_\infty$ the equilibrium curves $\langle \bar{c} \rangle_\tau = \bar{c}_\infty$ will be obtained instead of the equilibrium points. Figure 8 shows these equilibrium curves for $\bar{c}_\infty = 0.12$, $\Delta P = 1.5 \times 10^5$ Pa. The amounts of bubbles in the fractions are $N_1 = 3000$ and $N_2 = 7000$. The arrows show the direction of initial radius alteration (growth or dissolution of bubble): thick arrows are for the first fraction, thin arrows are for the second fraction. One can see that the equilibrium curves of different fractions cross when $a_{01} = a_{02}$ (the case of monodisperse cluster). Thus there are three different scenarios for a given initial gas concentration in the liquid:

(a) the bubbles in both fractions will dissolve (this is implemented in a very small region, not visible in the figure, where the initial bubble radii in both fractions less than 1 mkm);
(b) the bubbles of one fraction will dissolve or grow until they disappear, while the bubbles of another fraction converge to its equilibrium radius;
(c) the bubbles of both fractions will tend to the same radius.

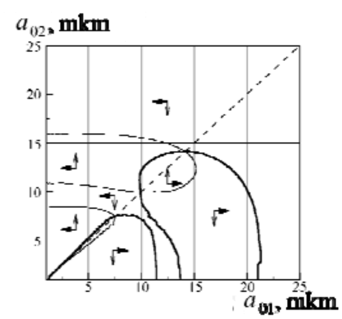

Figure 8: The equilibrium curves for bubbles in two-fraction cluster for $\bar{c}_\infty = 0.12$.

CONCLUSION

In this paper a mathematical model of bubble cluster is presented that allows studying:

- overall dynamics of the cluster as single mechanical object driven by external acoustic field;
- dynamics of individual bubbles inside the cluster;
- bubbles of different radii in the cluster and their interaction;
- gas diffusion between bubbles and liquid in the cluster.

The ranges of parameters of applicability of this model have been determined. The analytical study of small bubble oscillations based on the bubble cluster model proposed in this paper showed that the natural frequency of bubble oscillations in a monodisperse cluster is lower than the natural frequency of a single bubble (Minnaert frequency) with the same initial radius. It was also found that in a two-fraction cluster the secondary resonance in addition to the main resonance is present. In the range of the main resonance bubbles of different fractions oscillate in phase whereas in the range of the secondary resonance they oscillate out of phase.

The numerical analysis of nonlinear bubble oscillations in a polydisperse cluster revealed synchronization of the collapse phases of bubbles with different radii and collapse intensification for bubbles of one size in the presence of bubbles of other size.

The study of gas diffusion between bubble and liquid has shown that the diffusion stability of bubbles in a monodisperse cluster differs from the one for a single bubble in an infinite liquid. Namely an equilibrium radius in a cluster may be observed at higher values of dissolved gas concentration than for a single bubble. It means that a bubble in a monodisperse cluster is more diffusively stable than a single bubble. The numerical study of the diffusion in two-fraction cluster shows that the cluster has a tendency to become monodisperse or to disappear under the action of the acoustic field.

ACKNOWLEDGMENTS

This research is supported by the Ministry of Education and Science of the Russian Federation (Grant 11.G34.31.0040) and the Russian Foundation for Basic Research (Grant 11-08-00823-a).

REFERENCES

[1] Wijngaarden, L. van 1964, “On the collective collapse of a large number of cavitation bubbles in water,” *Proc. 11th International Congress of Applied Mechanics*, Munich, Springer Verlag (ed. H. Gortler), p. 854.

[2] Hansson, I., Kedrinskii, V.K., Morch, K.A. 1982, “On the dynamics of cavity clusters,” *J. Phys. D: Appl. Phys*., Vol. 15, p. 1725.

[3] Omta, R. 1987, “Oscillations of a cloud of bubbles of small and not so small amplitude,” *J. Acoust. Soc. Am*., Vol. 82, p. 1018.

[4] Chahine, G.L., Duraiswami, R. 1992, “Dynamical interaction in a multi-bubble cloud,” *J. Fluids Eng*., Vol. 114, p. 680.

[5] Kumar, S., Brennen, C.E. 1993, “Some nonlinear interactive effects in bubbly cavitation clouds,” *J. Fluid Mech*., Vol. 253, p. 565.

[6] Takahira, H., Akamatsu, T., Fujikawa, S. 1994, “Dynamics of a cluster of bubbles in a liquid (Theoretical analysis),” *JSME Int. J*., Ser. B., Vol. 37, No. 2, p. 297.

[7] Foldy L.L. 1945, “The multiple scattering of waves. I. General theory of isotropic scattering by randomly distributed scatterers,” *Phys. Rev*., Vol. 67, p. 107.

[8] Nigmatulin, R.I., Akhatov, I.S., Vakhitova, N.K., Nasibullayeva, E.Sh. 2000, “Dynamics of bubble clusters”, *Nonlinear Acoustics at the Turn of Millenium*, AIP conference proceedings, New York, Vol. 524, p. 455.

[9] Nasibullaeva, E.Sh., Akhatov, I.S. 2005, “Dynamics of a bubble cluster in an acoustic field,” *Acoustical Physics*, Vol. 51, No. 6, p. 705.

[10] Hairer, E., Norsett, S.P., Wanner, G. 1987, *Solving ordinary differential equations I. Nonstiff Problems*, Berlin: Springer-Verlag Berlin Heidelberg.

[11] Voronin, D.V., Sankin, G.N., Teslenko, V.S., Mettin, R., Lauterborn, W. 2003, “Secondary acoustic waves in a polydisperse bubbly medium,” *Journal of Applied Mechanics and Technical Physics*, Vol. 44, p. 17.

[12] Fyrillas, M.M., Szeri, A.J. 1994, “Dissolution or growth of soluble spherical oscillating bubbles,” *J. Fluid Mech*., Vol. 277, p. 381.

[13] Akhatov, I., Gumerov, N., Ohl, C.-D., Parlitz, U., Lauterborn, W. 1997, “The role of surface tension in stable single-bubble sonoluminescence,” *Ph. Rev. Lett*., Vol. 78, No. 2, p. 227.

[14] Akhatov, I., Konovalova, S. 2005, “Structure formation in acoustic cavitation,” *Multiphase Science and Technology*, Vol. 17, No. 3, p. 343.

[15] Nasibullaeva, E.Sh., Akhatov, I.S. 2007, “Diffusion stability of bubbles in a cluster,” *Journal of Applied Mechanics and Technical Physics*, Vol. 48, No. 4, p. 501.